Polarization anisotropy dynamics for thin films of a conjugated polymer aligned by nanoimprinting

S. A. Schmid,[1] K. H. Yim,[2] M. H. Chang,[1] Z. Zheng,[3] W. T. S. Huck,[3] R. H. Friend,[2] J. S. Kim,[2,*] and L. M. Herz[1,†]
[1]*Clarendon Laboratory, Department of Physics, University of Oxford, Parks Road, Oxford OX1 3PU, United Kingdom*
[2]*Optoelectronics Group, Cavendish Laboratory, University of Cambridge, Madingley Road, Cambridge CB3 0HE, United Kingdom*
[3]*Melville Laboratory for Polymer Synthesis, Department of Chemistry, University of Cambridge, Lensfield Road, Cambridge CB2 1EW, United Kingdom*

(Received 29 November 2007; revised manuscript received 8 February 2008; published 20 March 2008)

Time-integrated and femtosecond time-resolved photoluminescence spectroscopy has been used to study the dynamic emission polarization anisotropy for thin films of a conjugated polymer whose chains had been aligned through a nanoimprinting technique. The results indicate a high degree of chain alignment, with the presence of a small fraction of unaligned chain domains in film regions far from the imprinted surface. The time-averaged emission from aligned domains is found to be slightly shifted to higher photon energies compared to that from more disordered film regions. This effect is attributed to a subtly different chain packing geometry in the more aligned regions of the film, which leads to a reduced exciton diffusivity and inhibits energetic relaxation of the exciton in the inhomogeneously broadened density of states. While for an unaligned reference film, exciton migration results in a nearly complete depolarization of the emission over the first 300 ps, for the aligned films, interchain exciton hopping from unaligned to aligned domains is found to increase the anisotropy over the same time scale. In addition, excitons generated in aligned film domains were found to be slightly more susceptible to nonradiative quenching effects than those in disordered regions deeper inside the film, suggesting a marginally higher defect density near the nanoimprinted surface of the aligned film.

DOI: 10.1103/PhysRevB.77.115338 PACS number(s): 78.30.Jw, 78.66.Qn, 78.55.−m

I. INTRODUCTION

Since the first observation of electroluminescence in conjugated polymers,[1] these materials have attracted much interest from the scientific and industrial communities, as they exhibit the advantages of mechanical flexibility and low-cost processing techniques. Conjugated polymers have been successfully used as active layers in organic thin-film devices such as light-emitting diodes (LEDs),[2,3] photovoltaic cells,[4,5] and field effect transistors.[6,7] The strong delocalization of π electrons along the polymer backbone may introduce a uniaxial anisotropy to the electronic and optical properties of thin polymer films, allowing their implementation in polarized LEDs as backlighting for more efficient liquid-crystal displays. However, in thin films commonly produced by spin or drop casting techniques, conformational disorder of the polymer chains generally leads to fairly anisotropic optoelectronic properties of the film. Conjugated polymers exhibiting a liquid-crystalline phase, as, for example, poly(9,9-dioctylfluorene-*co*-benzothiadiazole) (F8BT), can be used to overcome structural disorder to a certain degree, as they have a tendency to form domains in which chains are aligned on a microscopic scale.[8,9] To extend such chain alignment into monodomains of a macroscopic scale, a whole range of techniques has been developed, including the usage of alignment layers consisting of mechanically rubbed[10,11] or photoaligned polyimide.[12] Another way of inducing a high degree of chain alignment is through tensile drawing of the thin polymer film, during which the chains become oriented along the drawing direction.[13] Recently, a new method has been developed to produce highly oriented conjugated polymer films through nanoimprinting.[14] Here, a stamp with nanometer-scale grooves is impressed onto the film that is heated to above its glass transition temperature, during which confinement of the chains in the nanochannels seeds the formation of a macroscopic domain of aligned polymer chains.

We have investigated the optical emission and absorption anisotropy of thin films of F8BT that have been subjected to the nanoimprinting technique to induce a high degree of chain alignment. Time-resolved and polarization-sensitive photoluminescence (PL) spectroscopy is used to trace the migration of excitations between different domains of the film, while emission-energy-sensitive anisotropy measurements are employed to elucidate the effect of the alignment process on the chain packing and the introduction of nonradiative defects.

II. EXPERIMENT

The samples investigated were made from F8BT, which is a green-light-emitting liquid-crystalline polymer that is relatively stable under exposure to air. Thin ($\sim$70 nm) films were prepared by spin coating a solution of F8BT (M_n $\sim$9000 g/mol) in *p*-xylene onto clean quartz substrates. Uniaxial alignment of the polymer chains was achieved through confinement of the material during nanoimprinting, which has been described in detail elsewhere.[14] Initially, a silicon mold with uniaxial oriented nanochannels of 20 nm width and interchannel spacing of 100 nm was assembled on top of the film. The sample was then heated above its glass transition temperature ($T_g \sim 90$ °C) to 160 °C, with the mold pressed onto the film for approximately 5 min. The arrangement was permitted to cool to 70 °C before the pressure was released. As previously demonstrated,[14] above T_g, the polymer is able to flow into the nanochannels with a concomitant alignment of the chains in the imprinting direc-

tion that is maintained after cooling. In addition, thin films of F8BT that had not been subjected to any alignment or annealing procedure were prepared as reference samples. After processing in air, the samples were stored in a dry-nitrogen glovebox outside the times of measurement.

To investigate the excitation dynamics in the films, time-resolved spectroscopy was conducted using the PL up-conversion technique.[15] The setup was based on a mode-locked Ti:sapphire laser, which supplied pulses of 100 fs duration at a repetition rate of 80 MHz. The frequency-doubled output at a photon energy of 2.755 eV was focused onto the sample for excitation with a fluence below 250 μW per 0.2 mm^2 excitation area to avoid degradation of the film during the measurement. A pair of off-axis parabolic mirrors collected the PL emitted from the sample in the forward direction (excitation incident on the imprinted surface of the polymer film) and focused it onto a nonlinear β-barium-borate (BBO) crystal held on a rotation stage. A vertically polarized gate beam at the laser fundamental (1.378 eV) was focused onto this crystal to overlap with the image spot of the collected PL. The crystal was rotated automatically to the angle at which phase matching permitted the formation of sum-frequency photons, which were collected, coupled into a monochromator, and detected by a liquid-nitrogen cooled charge coupled device. For time-resolved measurements of the PL, the relative time of arrival of the gate pulse was adjusted by changing the path length of the beam in the system with a computer-controlled delay stage. The phase-matching conditions at the BBO crystal are such that only the vertically polarized component of the collected PL was up-converted, while the polarization of the excitation beam could be selected by the rotation of a $\lambda/2$ plate and a Glan–Thompson polarizer. The temporal resolution of the system was determined by measuring the duration of the scattered excitation pulse to be ~300 fs. For measurements of the time-integrated PL originating from the sample, the gate beam was blocked and the BBO crystal was exchanged with a Glan–Thompson polarizing prism. The spectral response of the setup was measured using a tungsten filament lamp of known emissivity and has been corrected for on all spectra shown. To improve the signal-to-noise ratio and to compensate for potential spatial inhomogeneties of the samples, all measurements were repeated at several randomly distributed positions on the films, and the resulting curves were averaged. All experiments were conducted at room temperature with the samples placed in a vacuum chamber and kept at a pressure below 10^{-6} mbar to avoid photo-oxidation. Absorption spectra were taken using a spectrophotometer (Perkin Elmer, Lambda 9), with polarizers inserted into the sample and the reference beam path to select the polarization of the incident light.

III. RESULTS AND DISCUSSION

An initial assessment of the degree of chain alignment in the nanoimprinted samples may be obtained from the thin-film transmission spectra displayed in Fig. 1. Broad and featureless absorption spectra are observed for both parallel and perpendicular polarizations of the transmitted light with respect to the alignment axis. In both cases, the peak of absorption associated with the π-π^* transition of F8BT can be located at ~2.67 eV. The dichroic ratio between the absorbances, $D=A_{\parallel}/A_{\perp}$, was determined at the same energy to be $D=7$, which is in agreement with previously published work on almost identical samples.[14] Since the lowest transition dipole moment for most conjugated polymers tends to be preferentially oriented along the long axes of the chain, the measured dichroic ratio indicates a high degree of alignment in the sample. The residual absorption of light polarized perpendicular to the alignment axis may be caused either by the transition dipole moment forming a nonzero angle with the chain axis or by an imperfect alignment of the chains. As we will show in detail below, the nanoimprinted film still contains domains of unaligned polymer, indicating that the dichroic ratio observed for this sample is a lower limit of what is achievable through this technique. The inset in Fig. 1 demonstrates that the normalized spectra have a very similar shape, suggesting that the distributions of chain lengths and transition energies of the excited states for aligned and unaligned domains are similar.

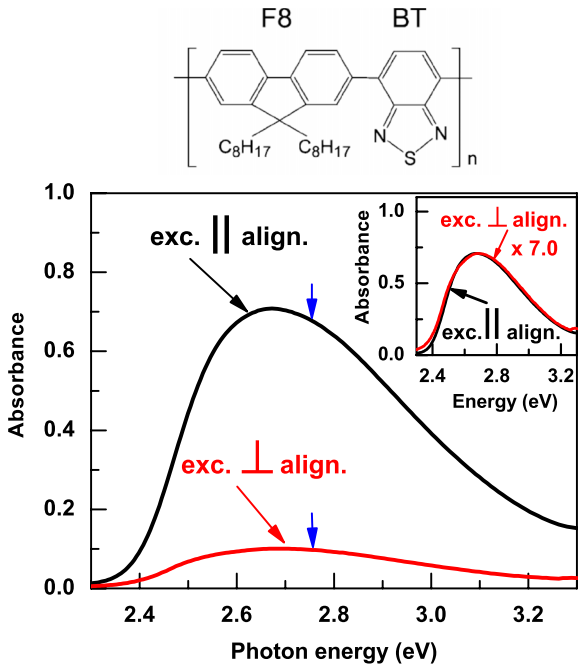

FIG. 1. (Color online) Top: Chemical structure of F8BT. Bottom: Absorption spectra for a nanoimprinted F8BT sample for the polarization of the excitation beam oriented parallel (black) and perpendicular (red) to the alignment axis. The inset shows both spectra normalized to the same peak value. The excitation energy used for time-integrated and time-resolved PL measurements is indicated with a vertical arrow.

To investigate the anisotropic character of the nanoimprinted thin films, time-integrated PL polarization spectra were taken and compared to those obtained from the reference sample that had not been subjected to the nanoimprinting treatment. For the isotropic reference film, the emitted PL components polarized parallel and perpendicular to the excitation polarization were measured. For the aligned samples, however, the alignment axis represents an addi-

tional degree of freedom, leading to four different configurations of detection polarizations with respect to the excitation polarization and alignment direction. These are schematically shown at the top of Fig. 2 and will be referred to in the following as configurations I–IV.

Figure 2(a) shows the time-integrated PL spectra of the reference film for the detection polarizations parallel and perpendicular to the excitation polarization, both of which exhibit emission peaks at around 2.30 and 2.17 eV. It has been suggested that these peaks are not simply caused by different vibrational transitions accompanying the same electronic transition but may, instead, be related to two distinct emissive states whose relative intensity is related to the chain packing structure adopted in the thin film.[14,16] The PL polarization ratio is given by the ratio of the PL intensities polarized parallel and perpendicular to the excitation polarization, $R=PL_{\parallel}/PL_{\perp}$, and is found to be $\sim$1.4 at the peak of the PL emitted from the reference sample. For a homogeneous distribution of randomly oriented transition dipole moments, a polarization ratio of 3.0 is theoretically expected directly after excitation.[17] As we will show in detail later, exciton migration processes from the initially excited polymer chains to neighboring chains of different orientations are the main cause of the low polarization ratio observed for the time-integrated measurements. Figure 2(b) displays the PL spectra for the aligned sample for the four different detection geometries illustrated at the top of the figure. As expected, the most intense emission occurs for excitation and detection polarizations parallel to the alignment direction (configuration I), and the smallest for both polarizations perpendicular to it (configuration IV). The PL intensity ratio for these two extreme cases, $PL_I/PL_{IV}\sim 16$, is similar to that previously reported for similar samples.[14] However, as these films are relatively thin, this ratio may be partly influenced by the fact that a different fraction of the total incident photons is absorbed by the film for excitation polarizations parallel and perpendicular to the alignment direction. Therefore, in the following, we will only consider polarization ratios and PL anisotropy values for sets of data taken for the same orientation of the excitation polarization with respect to the alignment direction. For example, for the excitation polarization parallel to the alignment direction, we find $R_{parallel}=PL_I/PL_{III}\sim 9$, whereas for the perpendicular case, $R_{perp}=PL_{II}/PL_{IV}\sim 4$ at the peak of the spectrum. The spectral dependence of this emission anisotropy will be discussed in more detail below.

To investigate the spectral changes in the emission with variation in the excitation and detection configuration, the PL spectra were normalized to their peak values, as shown in the insets in Figs. 2(a) and 2(b) for the reference and aligned samples, respectively. As expected, the isotropic reference film yields nearly identical spectral shapes for emission polarizations parallel and perpendicular to that of the excitation. In contrast, the PL peak emission energy for the aligned sample shows small but clearly resolvable shifts with measurement configurations—it decreases from 2.31 eV for configuration I to 2.29 eV for configuration III. The peak emission energy is higher for the two configurations with the emission polarized parallel to the alignment direction (I and II) than for the two configurations with the emission polar-

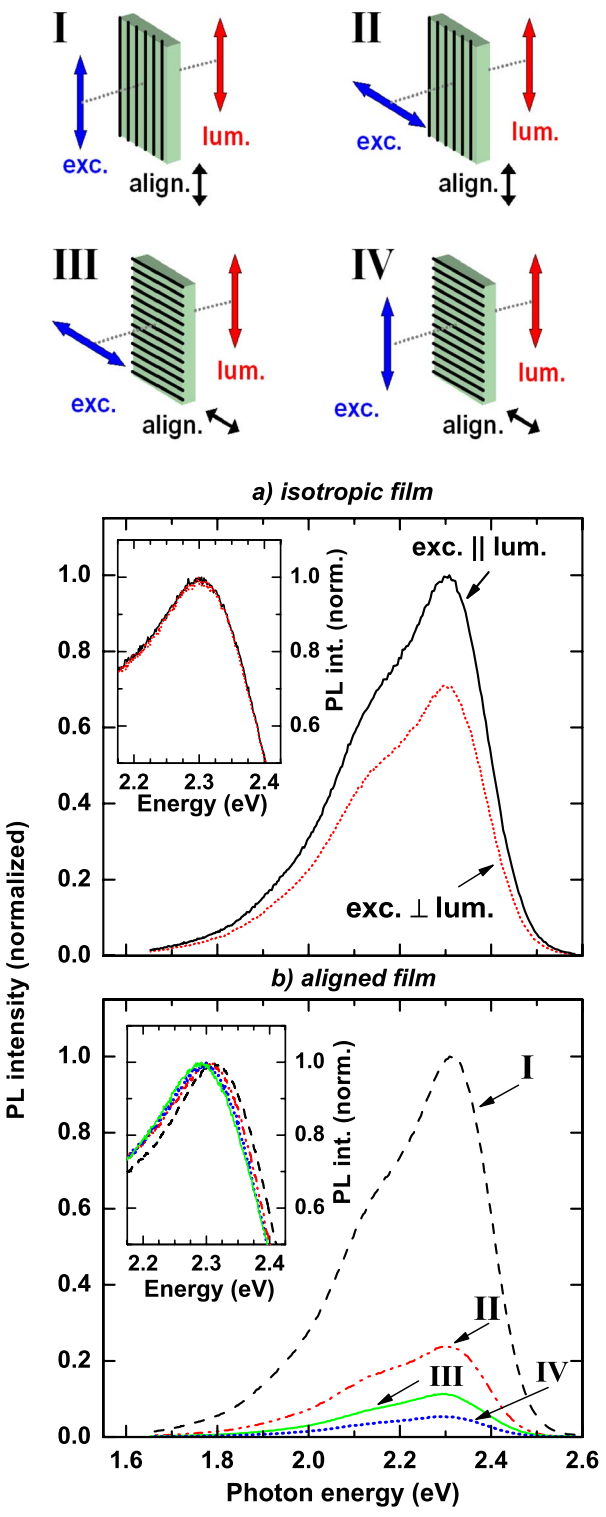

FIG. 2. (Color online) Top: Schematics of the four possible configurations for PL spectroscopy of the aligned sample. The excitation polarization and the detection polarization may be oriented either parallel or perpendicular to the alignment direction, resulting in the four configurations shown. Bottom: Time-integrated PL spectra for (a) an isotropic film of F8BT, with the detection polarization either parallel (solid black line) or perpendicular (red dotted line) to the excitation, and (b) an aligned film for the four configurations indicated at the top of the figure. The insets in (a) and (b) display the peak regions of the normalized PL spectra.

ized perpendicular to the alignment direction (III and IV). These measurements suggest that excitonic emission from the aligned chains is generally associated with marginally higher transition energies compared to that originating from the background of unaligned chains. This behavior is somewhat surprising since one might generally assume that the annealing and alignment of the polymer lead to an increased order and a reduced interchain separation associated with increased intermolecular electronic delocalization and a redshift in the emission.[18] However, it is consistent with recent observations of significant blueshifts in the emission from F8BT (Refs. 19 and 20) and poly(*p*-phenylenevinylene) (Refs. 21 and 22) upon annealing the films. A detailed study employing a wide range of experimental and theoretical techniques has recently concluded that for F8BT, these blueshifts are the result of a change in the chain packing structure upon annealing.[19] During the fast spin-coating process, the polymer chains are unable to adopt an optimized packing procedure, and the relatively large torsion angle between the F8 and BT units may lead to a chain arrangement, for which the BT units of neighboring chains are preferentially placed adjacent to one another. However, the strong local dipole on the monomer unit in F8BT (Ref. 23) dictates a low-energy packing geometry in which the BT units in one polymer chain are adjacent to the F8 units in the neighboring chain. Annealing facilitates the formation of such an "alternating" packing structure by allowing the BT units in adjacent chains to move away from one another.[19] The rearrangement to the alternating geometry has a profound effect on the optical and electronic properties of F8BT because of the strong confinement of the electron in the lowest unoccupied molecular orbital level on the BT unit. Quantum chemical calculations indicate that this localization restricts the electron mobility not only along the chain but also between adjacent chains, unless the BT units are aligned.[24] While the calculated hole wave function is more delocalized, the effect of electron localization still leads to similar effects for the calculated optical coupling and excitonic transfer rates between chains.[24] As a result, exciton migration should be reduced for the alternating chain arrangement adopted after annealing, leading to an inhibited relaxation of the exciton to lower-energy sites in the inhomogeneous distribution and a blueshift in the time-integrated emission. Note that this situation does not imply that annealed chains generally sustain higher-energy excitations but, rather, that the randomly generated excitons over time sample a higher-energy subset of the available states than they would in an unannealed film. For the aligned sample, those film domains that emit light preferentially polarized along the direction of the alignment stamp have generally undertaken the strongest chain movement during annealing and, therefore, are more likely to have adopted the alternating chain packing structure. As a result, the time-integrated emission polarized parallel to the alignment direction should be shifted to higher energies, as observed.

It has been shown that the introduction of one-dimensional nanostructures on a polymer film can lower the glass transition temperature in this region.[25] The alignment of chains through nanoimprinting may then occur from the stamp surface onward, as suggested by a measured decrease in the uniaxial order parameters for these films with increasing film thickness.[14] As a result, the films are likely to exhibit a strong chain alignment near the front (imprinted) surface, with more disordered domains nearer the back surface of the film. However, the imprinting process may also lead to a higher defect concentration near this interface, e.g., through prolonged exposure of the front surface of the film to air. Therefore, an alternative explanation for the blueshifted emission from aligned chains is that a higher concentration of nonluminescent traps in the aligned domains near the surface leads to a faster exciton quenching here than in the regions deeper in the film. This would be compatible with the shorter emission lifetimes found for aligned chains (*vide infra*) and could also result in a blueshifted emission by reducing the time available for an exciton to energetically relax. Recent investigations of F8BT layers deposited on a thin hole transporting layer have shown that quenching of excitons at the interface between the two more severely affected the lower-energy peak of the F8BT emission near 2.17 eV than the higher-energy peak, leading to a net blueshift in the emission.[16]

To investigate the emission anisotropy induced through the nanoimprinting technique, the PL polarization anisotropy r was calculated from the relevant PL spectra as

$$r(E) = \frac{I_{\parallel}(E) - I_{\perp}(E)}{I_{\parallel}(E) + 2I_{\perp}(E)}, \tag{1}$$

Here, $I_{\parallel}(E)$ $[I_{\perp}(E)]$ is the PL intensity polarized parallel (perpendicular) to the excitation polarization at given photon energy E. Figure 3 shows $r(E)$ for the reference sample [Fig. 3(b)] and for the aligned sample both for the case of the excitation polarization parallel [Fig. 3(a)] and perpendicular [Fig. 3(c)] to the alignment direction.

For the isotropic reference film the emission anisotropy is generally low and decreases monotonically toward lower energies similar to previously observed trends for other conjugated polymers.[26] In conjugated polymers, disorder leads to a wide variation in the lengths of the conjugated segments with a corresponding inhomogeneously broadened density of states (DOS) of the excitons. During their lifetime, excitons gradually migrate to longer segments with lower energies within the DOS, leading to a redshift in the peak energy of the emission.[27–29] Incoherent hopping of the exciton from segment to segment will also lead to a rotation of the excitonic dipole moment if the segments are oriented at a nonzero angle with respect to one another. As a result, excitons emitting at lower photon energies are more likely to have undertaken a significant number of hops between segments and to have lost a large fraction of the original polarization memory than those emitting from shorter segments at higher photon energies. The dynamics of this emission depolarization will be discussed in more detail below.

For the excitation of the aligned film with polarization parallel to the alignment direction [Fig. 3(a)], the emission anisotropy is high ($r \geq 0.7$) at all photon energies, confirming the strong degree of alignment achieved with the nanoimprint technique. The emission anisotropy spectrum shows a distinct derivativelike feature centered near 2.3 eV, which is related to the peak shifts observed in the PL spectra measured for configurations I and III, as discussed above. The

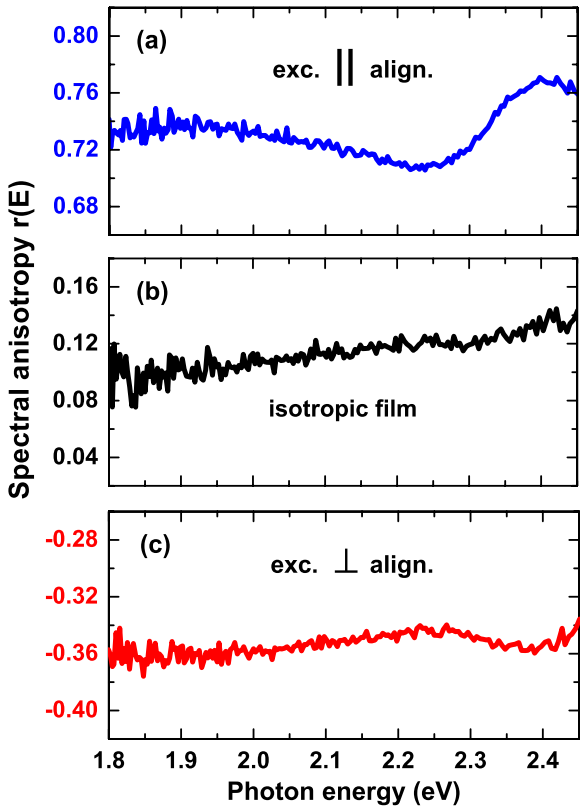

FIG. 3. (Color online) Polarization anisotropy spectra for the time-integrated emission from the aligned film for the case of the excitation polarization oriented (a) parallel and (c) perpendicular to the direction of alignment and (b) for the isotropic reference film.

sharpness of this feature is qualitatively different from the gradual decrease with photon energy observed for the isotropic sample. It appears that for the aligned sample, an inhibition of exciton migration through either a rearrangement of the chain packing geometry or trapping at defects near the surface affects the two emission peaks near 2.17 and 2.3 eV to a different extent, which is in agreement with previous exciton quenching studies on F8BT.[16] Similar effects have recently been observed in the emission anisotropy spectra of aligned films of poly(phenylene vinylene), for which they have similarly been attributed to the presence of two emitting states associated with the amorphous and crystalline regions of the film.[26] For the excitation polarized perpendicular to the alignment direction [Fig. 3(c)], the polarization anisotropy is negative at all photon energies, indicating that the emission component polarized parallel to the alignment direction (i.e., $I_{\perp}$, since it is polarized perpendicular to the excitation polarization) is always larger than that polarized perpendicular to the alignment direction ($I_{\parallel}$), again indicating the high degree of order achieved. Interestingly, the emission anisotropy becomes more negative (increases in magnitude) with decreasing photon energy, suggesting a repolarization of the emission as excitons move through the DOS, corresponding to a move from unaligned to more aligned film domains over time.

The spectral dependence of the emission anisotropy suggests that the migration of excitons during their lifetime induces significant changes in the polarization anisotropy.

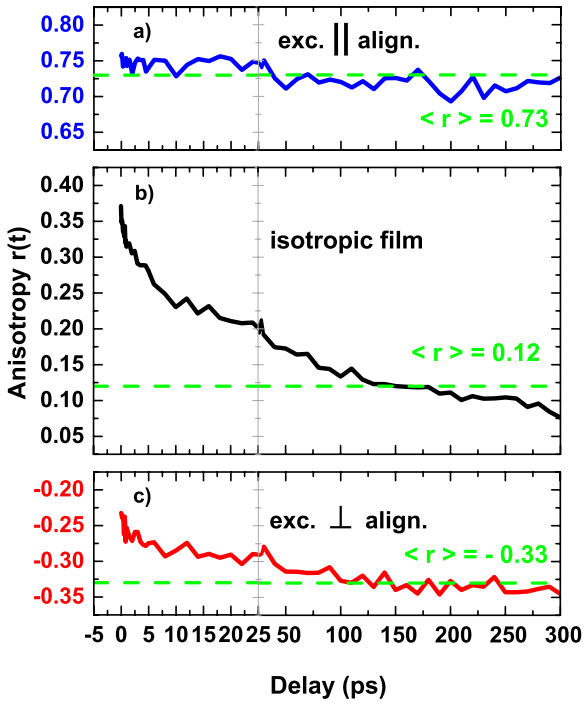

FIG. 4. (Color online) Time-resolved emission polarization anisotropy at a detection energy of 2.317 eV for the aligned film with the excitation polarization oriented (a) parallel and (c) perpendicular to the aligment axis and for (b) the isotropic reference film. The time-integrated anisotropy value $\langle r \rangle$ measured at the same energy is indicated by a dashed (green) line in each graph.

Therefore, in the following, we discuss the temporal evolution of the emission anisotropy $r(t)$ extracted from the measured photoluminescence decays for all samples. Figure 4 shows the PL polarization anisotropy $r(t)$ at a detection energy of 2.317 eV for the isotropic reference sample [Fig. 4(b)] and for the nanoimprinted film for the cases of excitation with polarization parallel [Fig. 4(a)] and perpendicular [Fig. 4(c)] to the alignment direction. The dashed line in Fig. 4 also indicates the time-integrated anisotropy values $r(E)$ extracted from Fig. 3 at 2.317 eV, which show an apparently good convergence with the time-dependent anisotropy curves.

For the reference film [Fig. 4(b)], the initial anisotropy $r(0)$ is ~0.37, which, within experimental error, is equal to the theoretical value of 0.4 for a randomly oriented distribution of noninteracting transition dipole moments of a two-level system.[17] This observation suggests that the chain segments in the reference sample have an orientation distribution that is close to being totally isotropic. Grazing angle PL measurements have indicated that high-molecular-weight F8BT forms films with chains preferentially aligned within the substrate plane, while low-molecular-weight samples such as those used for the films under investigation here had an almost isotropic chain orientation,[20] which is in agreement with our findings. It has recently been suggested that the initial polarization anisotropy may be significantly lower than 0.4 as a result of intramolecular[30,31] and intermolecular[32] delocalizations of the initially excited state. Here, intramolecular effects may originate from the presence

of fully conjugated but curved segments that induce an ultrafast (<100 fs) depolarization of the emission as a result of exciton localization following a geometric relaxation of the chain.[30,31] In contrast, intermolecular effects may result from a strong electronic coupling between adjacent chains that leads to a splitting of the excited electronic state and may induce an ultrafast rotation of the transition dipole moment through relaxation between the split upper electronic state.[32] Therefore, the observed value of $r(0) \sim 0.4$ suggests that neither chain bending nor interchain interactions within the strong coupling regime are important for F8BT. After excitation, the emission polarization anisotropy rapidly decays, which is consistent with an incoherent hopping transfer of excitations between sites of different transition dipole orientations.[33] A fast initial decrease in $r(t)$ from 0.37 to 0.30 can be observed within the first 2 ps and is followed by a slower decay at later times [$r(25\ \text{ps}) \sim 0.20$] as excitons relax within the DOS and the site-to-site transfer rate decreases. The nearly complete depolarization for long times after excitation [$r(300\ \text{ps}) \sim 0.07$] suggests that excitations are able to migrate over large distances compared to the typical interchain separation in the film,[34] which is in agreement with the relatively large diffusion range of 10–15 nm previously estimated for short-chain F8BT (about six average repeat units).[16]

For the aligned film, the PL depolarization dynamics differ significantly from the isotropic case. For the excitation polarized perpendicular to the alignment direction [Fig. 4(c)], the initial anisotropy has a negative value of −0.23, which means that the emission immediately after excitation is more strongly polarized along the alignment direction than perpendicular to it [see Eq. (1)]. Within the first 2 ps following excitation, a fast growth in the magnitude of the anisotropy to −0.27 can be observed, followed by a much slower increase in magnitude to −0.34 at 300 ps after excitation. The temporal evolution of anisotropy is thus similar to that in the spin-cast film, but with the interesting difference that $r(t)$ becomes more and more negative with increasing time. These results strongly suggest that while the excitation polarized perpendicular to the alignment direction leads to the creation of a fraction of excitons on unaligned domains, there is a net migration from these to more aligned domains in the film, leading to an increase in emission polarized parallel to the alignment direction. In contrast, the excitation polarized parallel to the alignment direction leads to a high initial anisotopy ~0.76 [Fig. 4(a)] that only marginally decays [$r(300\ \text{ps}) \sim 0.72$] over the observed time range. These dynamics show that because of the high degree of alignment, the unaligned chains form the minority of available sites in the film, making exciton diffusion from unaligned to aligned domains more likely than the reverse process. Therefore, exciton migration is a process enhancing the emission polarization in highly aligned films, which is in agreement with similar observations previously made for polyfluorene films prepared through a rubber-aligned substrate layer.[35]

Finally, we discuss the effect that alignment through nanoimprinting has on the presence of defect quenchers in the material. For this purpose, we have examined the lifetime of excitations in the reference and the nanoimprinted films. Figure 5 shows the temporal decay of the total photoluminescence $I_{total}(t) = I_{\parallel}(t) + 2I_{\perp}(t)$, where $I_{\parallel}$ and $I_{\perp}$ are the components polarized parallel and perpendicular to the excitation polarization, as in previous sections. Superimposed on these data are monoexponential fits over the time period from 50 to 300 ps. The PL decay for the reference film and that for the aligned film after the excitation polarized perpendicular to the alignment directions of the aligned sample are very similar: Both show a nearly monoexponential behavior with decay constants near 550 ps. In contrast, the PL decay for the aligned film after excitation polarized parallel to the alignment direction deviates from a monoexponential decay, containing a small faster decaying component within the first 50 ps. The ensuing decay over the next 250 ps has a time constant of ~450 ps, which is about 10% lower than that for the other two cases. Therefore, it appears that the PL emerging from the aligned domains of the nanoimprinted film is associated with a shorter excitonic lifetime that is connected with a stronger presence of nonradiative quenching sites. Since the nanoimprinting process was carried out in air with the imprinted side being more strongly exposed, a prevalence of oxidated quenching sites near the more aligned top region of the sample is very likely. It is, for example, known that fluorene units are susceptible to C=O defect formation through photo-oxidation,[36] which will act as luminescence quenchers resulting in nonexponential decay dynamics and a general reduction in excitation lifetime.[35,37] It has been shown that such photo-oxidation more strongly affects the air-exposed side of a film than the side facing the substrate.[38] In this case, the stronger susceptibility of the aligned domains to exciton quenching is simply the result of their proximity to the sample surface as the exciting light polarized parallel to the alignment direction will experience a higher absorption coefficient than it would in an unaligned film. Measurements of charge mobility in top-gate field effect transistors fabricated with unaligned and nanoimprinted F8BT films that probe the same sample depth from the surface (i.e., the charge accu-

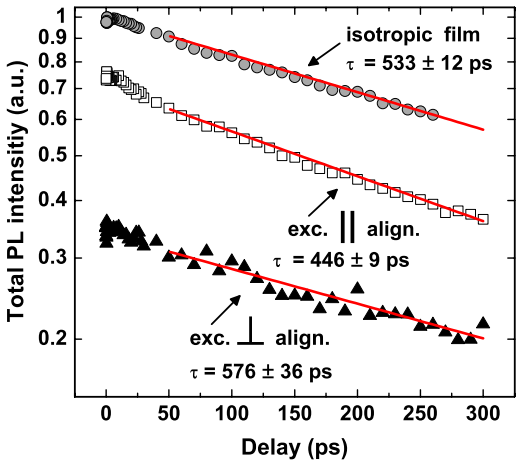

FIG. 5. (Color online) Total PL intensity dynamics at 2.317 eV for the isotropic reference film (gray circles) and for the aligned film for the excitation polarized parallel (open squares) and perpendicular (black triangles) to the alignment direction. For each decay curve, monoexponential fits (solid red lines) to the data from 50 ps onward are displayed with the extracted lifetime τ, as indicated. The curves have been rescaled for clarity.

mulation layer), but for charge carriers rather than excitons, have not indicated a detrimental effect of the nanoimprinting procedure.[14] It should be noted that the differences in the overall PL decay dynamics are very subtle, suggesting that the introduced surface defect density is low, and improvements could probably also be made through processing in an inert environment. Other alignment techniques, such as film stretching, have been shown to cause significant defect densities,[38] as evident from measured rapid PL decay dynamics. Therefore, nanoimprinting appears to be a versatile technique that allows the production of highly aligned films with relatively low defect densities.

IV. CONCLUSION

We have examined the polarization anisotropy in the optical absorption and emission from thin films of F8BT before and after treatment with a recently developed chain alignment procedure based on nanoimprinting.[14] While the as-spun reference film shows little anisotropy, the nanoimprinting treatment leads to strongly polarized absorption and emission, indicating a high degree of alignment of the polymer chains along the direction of the nanochannels. An analysis of the spectral dependence of the PL polarization anisotropy indicates that the emission from aligned polymer chains near the sample surface is blueshifted with respect to that from unaligned residual domains deeper inside the film. This effect is partly attributed to a different packing geometry adopted by the chains after annealing, which results in a planarization of the backbone and a preferential arrangement of BT units on one chain adjacent to F8 units on another chain, as recently proposed in a detailed study of conformational effects in F8BT.[19] The larger separation between BT units of neighboring chains then causes a reduced interchain exciton diffusivity and inhibits energetic relaxation of the exciton, leading to a blueshift in the emission at longer times after excitation, which manifests itself in the observed shifts in the time-averaged emission spectra. This does not imply that annealed chains generally sustain higher-energy excitations but, rather, that excitons migrating through the aligned regions of the film sample a higher-energy subset of the available states than those in unaligned regions, particularly at later times after excitation. Since the observed spectral shifts are at most 20 meV and, thus, smaller than kT at room temperature, these effects are unlikely to have a significant impact on the extent of exciton migration occurring between aligned and unaligned regions. As an alternative explanation, the presence of an increased nonradiative defect concentration near the sample surface resulting from the imprinting process may reduce the exciton lifetime on aligned domains and lead to a blueshift of the time-integrated excitation. The latter explanation is compatible with the shorter lifetime observed for emission polarized in the alignment direction. Time-resolved PL anisotropy measurements were conducted to investigate the dynamics of exciton migration between different domains of the films. For the pristine film, a nearly complete decay of the emission polarization anisotropy within the first 300 ps is observed, indicating efficient exciton hopping transfer through an isotropic distribution of randomly oriented conjugated segments. However, in the aligned sample, the emission anisotropy is found to gradually increase in magnitude for the excitation polarized perpendicular to the alignment direction and remains roughly constant for the case of parallel excitation polarization. We conclude that exciton migration from unaligned to aligned chains is significantly more likely than vice versa. For the investigated films, unaligned chains must therefore form minority domains inside the film, allowing exciton migration to augment the emission of polarized light. Both the exciton migration between different film regions and the existence of an off-axis transition dipole moment on the single chain of F8BT influence the magnitude of the residual unpolarized emission background and have to be taken into account for the accurate determination of order parameters.

ACKNOWLEDGMENTS

We thank Cambridge Display Technology (CDT) for the provision of F8BT. This work was funded through research grants awarded by the Engineering and Physical Sciences Research Council (United Kingdom) (EPSRC-GB). J.S.K. and L.M.H. are supported by the EPSRC-GB through the ARF Scheme. K.H.Y. and Z.Z. would like to thank CDT for funding, and Z.Z. would like to acknowledge funding support through an EPSRC-GB Dorothy Hodgkin Postgraduate Grant.

*Present address: Blackett Laboratory, Imperial College London, London SW7 2AZ, UK.

†l.herz1@physics.ox.ac.uk

[1] J. H. Burroughes, D. D. C. Bradley, A. R. Brown, R. N. Marks, K. Mackay, R. H. Friend, P. L. Burns, and A. B. Holmes, Nature (London) **347**, 539 (1990).

[2] P. K. H. Ho, J.-S. Kim, J. H. Burroughes, H. Becker, S. F. Y. Li, T. M. Brown, F. Cacialli, and R. H. Friend, Nature (London) **404**, 481 (2000).

[3] Y. Cao, I. D. Parker, G. Yu, C. Zhang, and A. J. Heeger, Nature (London) **397**, 414 (1999).

[4] J. J. M. Halls, C. A. Walsh, N. C. Greenham, E. A. Marseglia, R. H. Friend, S. C. Moratti, and A. B. Holmes, Nature (London) **376**, 498 (1995).

[5] A. C. Arias, N. Corcoran, M. Banach, R. H. Friend, J. D. MacKenzie, and W. T. S. Huck, Appl. Phys. Lett. **80**, 1695 (2002).

[6] L. L. Chua, J. Zaumseil, J.-F. Chang, E. C.-W. Ou, P. K.-H. Ho, H. Sirringhaus, and R. H. Friend, Nature (London) **434**, 194 (2005).

[7] H. Sirringhaus, P. J. Brown, R. H. Friend, M. M. Nielsen, K. Bechgaard, B. M. W. Langeveld-Voss, A. J. H. Spiering, R. A. J. Janssen, E. W. Meijer, P. Herwig and D. M. de Leeuw, Nature (London) **401**, 685 (1999).

[8] M. Grell, M. Redecker, K. S. Whitehead, D. D. C. Bradley, M.

Inbasekaran, E. P. Woo, and W. Wu, Liq. Cryst. **26**, 1403 (1999).
[9] H.-M. Liem, P. Etchegoin, K. S. Whitehead, and D. D. C. Bradley, Adv. Funct. Mater. **13**, 66 (2003).
[10] H. Sirringhaus, R. J. Wilson, R. H. Friend, M. Inbasekaran, W. Wu, E. P. Woo, M. Grell, and D. D. C. Bradley, Appl. Phys. Lett. **77**, 406 (2000).
[11] M. Grell, W. Knoll, D. Lupo, A. Meisel, T. Miteva, D. Neher, H.-G. Nothofer, U. Scherf, and A. Yasuda, Adv. Mater. (Weinheim, Ger.) **11**, 671 (1999).
[12] K. Sakamoto, K. Usami, Y. Uehara, and S. Ushioda, Appl. Phys. Lett. **87**, 211910 (2005).
[13] D. D. C. Bradley, J. Phys. D **20**, 1389 (1987).
[14] Z. Zheng, K.-H. Yim, M. S. M. Saifullah, M. E. Welland, R. H. Friend, J.-S. Kim, and W. T. S. Huck, Nano Lett. **7**, 987 (2007).
[15] M. H. Chang, M. J. Frampton, H. L. Anderson, and L. M. Herz, Appl. Phys. Lett. **89**, 232110 (2006).
[16] J. S. Kim, I. Grizzi, J. H. Burroughes, and R. H. Friend, Appl. Phys. Lett. **87**, 023506 (2005).
[17] B. Valeur, *Molecular Fluorescence: Principles and Applications* (Wiley-VCH, Weinheim, 2002).
[18] T.-Q. Nguyen, I. B. Martini, J. Liu, and B. J. Schwartz, J. Phys. Chem. B **104**, 237 (2000).
[19] C. L. Donley, J. Zaumseil, J. W. Andreasen, M. M. Nielsen, H. Sirringhaus, R. H. Friend, and J.-S. Kim, J. Am. Chem. Soc. **127**, 12890 (2005).
[20] K.-H. Yim, R. H. Friend, and J.-S. Kim, J. Chem. Phys. **124**, 184706 (2006).
[21] J. A. Mikroyannidis, I. K. Spiliopoulos, T. S. Kasimis, A. P. Kulkarni, and S. A. Jenekhe, Macromolecules **36**, 9295 (2003).
[22] J. A. Mikroyannidis, P. D. Vellis, P. I. Karastatiris, and I. K. Spiliopoulos, Synth. Met. **145**, 87 (2004).
[23] P. Sreearunothai, A. C. Morteani, I. Avilov, J. Cornil, D. Beljonne, R. H. Friend, R. T. Phillips, C. Silva, and L. M. Herz, Phys. Rev. Lett. **96**, 117403 (2006).
[24] J. Cornil, I. Gueli, A. Dkhissi, J. C. Sancho-Garcia, E. Hennebicq, J. P. Calbert, V. Lemaur, D. Beljonne, and J. L. Brédas, J. Chem. Phys. **118**, 6615 (2003).
[25] M. K. Mundra, S. K. Donthu, V. P. Dravid, and J. M. Torkelson, Nano Lett. **7**, 713 (2007).
[26] C. Soci, D. Comoretto, F. Marabelli, and D. Moses, Phys. Rev. B **75**, 075204 (2007).
[27] R. Kersting, U. Lemmer, R. F. Mahrt, K. Leo, H. Kurz, H. Bässler, and E. O. Göbel, Phys. Rev. Lett. **70**, 3820 (1993).
[28] G. R. Hayes, I. D. W. Samuel, and R. T. Phillips, Phys. Rev. B **52**, R11569 (1995).
[29] L. M. Herz, C. Silva, A. C. Grimsdale, K. Müllen, and R. T. Phillips, Phys. Rev. B **70**, 165207 (2004).
[30] A. Ruseckas, P. Wood, I. D. W. Samuel, G. R. Webster, W. J. Mitchell, P. L. Burn, and V. Sundström, Phys. Rev. B **72**, 115214 (2005).
[31] M. H. Chang, M. Hoffmann, H. L. Anderson, and L. M. Herz (unpublished).
[32] M. H. Chang, M. J. Frampton, H. L. Anderson, and L. M. Herz, Phys. Rev. Lett. **98**, 027402 (2007).
[33] Mette M.-L. Grage, Y. Zaushitsyn, A. Yartsev, M. Chachisvilis, V. Sundström, and T. Pullerits, Phys. Rev. B **67**, 205207 (2003).
[34] A. Ruseckas, M. Theander, L. Valkhunas, M. R. Andersson, O. Inganäs, and V. Sundström, J. Lumin. **76-77**, 474 (1998).
[35] L. M. Herz and R. T. Phillips, Phys. Rev. B **61**, 13691 (2000).
[36] V. N. Bliznyuk, S. A. Carter, J. C. Scott, G. Klärner, R. D. Miller, and D. C. Miller, Macromolecules **32**, 361 (1999).
[37] M. Yan, L. J. Rothberg, F. Papadimitrakopoulos, M. E. Galvin, and T. M. Miller, Phys. Rev. Lett. **73**, 744 (1994).
[38] G. R. Hayes, I. D. W. Samuel, and R. T. Phillips, Phys. Rev. B **56**, 3838 (1997).